Increased functional connectivity indicates the severity of cognitive impairment in multiple sclerosis

David J. Hawellek[a,1], Joerg F. Hipp[a,b], Christopher M. Lewis[c,d,e], Maurizio Corbetta[d,e,f], and Andreas K. Engel[a]

[a]Department of Neurophysiology and Pathophysiology, University Medical Center Hamburg-Eppendorf, 20246 Hamburg, Germany; [b]Centre for Integrative Neuroscience, University of Tübingen, 72076 Tübingen, Germany; [c]Ernst Stüngmann Institute in cooperation with The Max Planck Society, 60528 Frankfurt, Germany; [d]Department of Clinical Sciences and Bioimaging and [e]Institute for Advanced Biomedical Technologies, G. D'Annunzio University, 66100 Chieti, Italy; and [f]Departments of Neurology, Radiology, Anatomy and Neurobiology, Washington University School of Medicine, St. Louis, MO 63110

Edited by Marcus E. Raichle, Washington University, St. Louis, MO, and approved October 19, 2011 (received for review June 22, 2011)

Correlations in spontaneous brain activity provide powerful access to large-scale organizational principles of the CNS. However, making inferences about cognitive processes requires a detailed understanding of the link between these couplings and the structural integrity of the CNS. We studied the impact of multiple sclerosis, which leads to the severe disintegration of the central white matter, on functional connectivity patterns in spontaneous cortical activity. Using a data driven approach based on the strength of a salient pattern of cognitive pathology, we identified distinct networks that exhibit increases in functional connectivity despite the presence of strong and diffuse reductions of the central white-matter integrity. The default mode network emerged as a core target of these connectivity modulations, showing enhanced functional coupling in bilateral inferior parietal cortex, posterior cingulate, and medial prefrontal cortex. These findings imply a complex and diverging relation of anatomical and functional connectivity in early multiple sclerosis and, thus, add an important observation for understanding how cognitive abilities and CNS integrity may be reflected in the intrinsic covariance of functional signals.

resting state | BOLD fMRI | diffusion tensor imaging | fractional anisotropy | neurological

Understanding how disease processes affect functional interactions in the CNS is a core challenge of neuroscience research. fMRI connectivity has become an important tool for revealing large-scale network interactions by analyzing correlations in intrinsic fluctuations of the BOLD signal (1). This method is sensitive to plastic as well as developmental changes of the functional architecture (2–5), and has successfully linked specific cognitive syndromes to the pathology of distinct functional systems (e.g., spatial neglect after stroke, different forms of dementias, and healthy aging) (6–8). The structural wiring of the brain plays an essential role in shaping the spatial patterns of functional interactions (9, 10). However, the activity correlations are not fully determined by the anatomical connections and, thus, provide complementary information about network organization (11). Especially in the context of neurological damage, the functional covariance structure may document pathological effects well beyond focal damage, indicating the complex changes of interactions that occur in distributed networks (12–14). Commonly, the coupling strength of spontaneous brain activity is thought to be a direct proxy for the functioning of brain networks, with stronger interactions also reflecting a stronger computational capacity (15, 16).

In this study we have investigated how cognitive pathology due to neurological damage in multiple sclerosis (MS) is reflected in changes of structural and functional connectivity. Compared with other CNS pathologies, MS stands out due to the prominent involvement of the central white matter. During the disease process, the immune system exerts inflammatory insults to neuronal myelination and axonal integrity (17). These processes may lead to the loss of functional cofluctuations (18), especially in late and severe stages of the disease (19), reminiscent of a scenario of complete disconnection as in the extreme case of corpus callosotomy (20). Surprisingly, however, recent studies also report increased functional connectivity in earlier stages of the disease (21–23). This raises the question of how cognitive impairment that occurs as an early and prominent consequence of MS (24) may relate to changes of functional connectivity. A challenging aspect of the cognitive decline is the weak association between specific lesion parameters, such as the location of T2-visible plaques and circumscribed cognitive abilities (25, 26). It is becoming increasingly clear that subtle, nonfocal white matter damage (as assessed by, e.g., diffusion-weighted imaging) plays a crucial role in determining the presence and extent of cognitive impairment (27–30). Thus, the manner in which the disease affects cognition is likely not a collection of random and focal disturbances, but has widespread structural and functional consequences as an important pathological element (31).

In a group of early stage patients, we found the cognitive pathology to exhibit a salient multivariate pattern, a general factor. Further, we found this pattern of impairment to be related to the widespread integrity of the central white matter. Finally, by means of a data driven approach, we identified the default mode network to be central to strong modulations of functional connectivity by the severity of the cognitive pathology. Strikingly, the reduction in cognitive ability and widespread anatomical connectivity was associated with increased functional connectivity. These results reveal a dissociation of changes in functional and anatomical connectivity in relation to cognitive ability and add an important empirical observation for understanding how fMRI connectivity may index the integrity of cortical circuits. Our findings hold significant implications for resting state investigations of brain diseases as well as theoretical and modeling studies of large-scale cortical dynamics.

Results

Cognitive Efficiency. To assess the presence and structure of cognitive impairment, we quantified the performance of 16 patients in the early stages of MS (Table S1) and individually matched controls in a set of neuropsychological tests. All tests were standard tools used in clinical and research settings and together probed a broad range of different sensory, cognitive, and output modalities. Fig. 1*A* summarizes the test results for all patients, sorted such that the patient with the worst performance appears at the top and the test accumulating the most negative performance appears to the left. Three important features of the overall

Author contributions: D.J.H., J.F.H., M.C., and A.K.E. designed research; D.J.H. performed research; D.J.H., J.F.H., and C.M.L. analyzed data; and D.J.H., J.F.H., M.C., and A.K.E. wrote the paper.

The authors declare no conflict of interest.

This article is a PNAS Direct Submission.

Freely available online through the PNAS open access option.

[1]To whom correspondence should be addressed. E-mail: d.hawellek@uke.de.

This article contains supporting information online at www.pnas.org/lookup/suppl/doi:10.1073/pnas.1110024108/-/DCSupplemental.

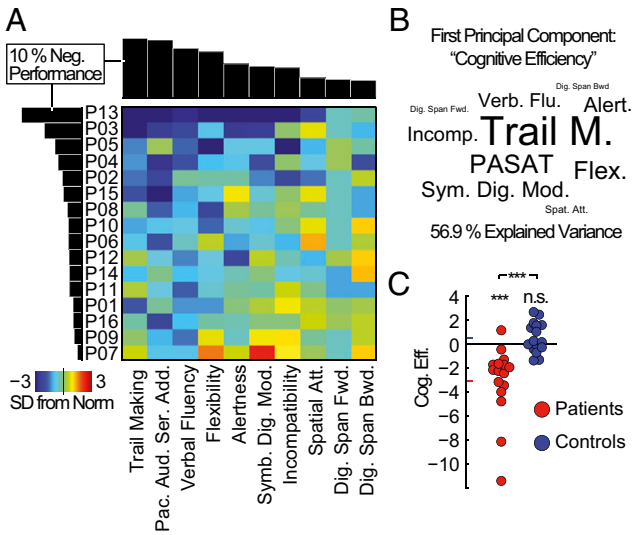

Fig. 1. Cognitive pathology is dominated by a general factor of cognitive functioning. (*A*) Neuropsychological test results for all patients (see Fig. S1 for the combined patient and control data set). The color code indicates deviations from the age and education norm in SDs. Both axes have been sorted by the percentage of overall negative performance, as shown in the margins. (*B*) Test name sizes scaled by the loadings of the first principal component for the combined patient and control dataset (spatial positioning is arbitrary). This component explained 56.9% of the overall variance in test performance and is referred to as cognitive efficiency in all subsequent analyses. (*C*) Component scores of the first principal component for all study participants. Group means are indicated by the colored bars at the ordinate.

pattern of cognitive pathology in the sample emerged. First, the cognitive impairment exhibited a considerable variability, with some patients showing only mild deficits and other patients being more severely affected. Second, some tests were particularly sensitive in uncovering negative performance early, suggesting that they tap into functions, which are especially prone to the disease process. And third, with increasing severity of the pathology, the impairment appeared to broaden across tests, successively spanning a wider range of tested modalities. Thus, instead of multiple, more-specific patterns of impairment, the patients mainly differed in the general bandwidth of cognitive processes, leading to the emergence of a general factor of cognitive pathology. To quantify and further analyze this pattern, we applied principal component analysis (PCA) to the behavioral performance of patients and healthy controls.

The first principal component of the test battery explained >50% of the total behavioral variance observed; it was the only pattern discernible from Gaussian noise ($P < 10^{-16}$), and robust to overfitting effects (Fig. S1 *B* and *C*). Importantly, all weights of the component had the same sign, again indicating the main feature of a general factor, i.e., the positive correlation of test performance across subjects. To give an idea of how each of the tests contributed to the component, Fig. 1*B* shows the test names scaled by the first component's eigenvector (loadings). The tests with a high impact (trail making, paced auditory serial addition test, and verbal fluency) had an emphasis on executive functions, speed of processing, and cognitive flexibility, and presumably require the dynamic integration of information in large-scale networks (32). The level of this general factor, hereafter referred to as cognitive efficiency, separated the patient and control group (Fig. 1*C*). The patient group showed a significant decrease in cognitive efficiency (difference from zero: *t* test, $P = 9.63 \times 10^{-4}$; group difference: paired *t* test, $P = 9.24 \times 10^{-4}$). The healthy control group did not differ from the norm level of cognitive efficiency (*t* test, $P = 0.101$). A classification into patients and controls based on cognitive efficiency yielded a sensitivity of up to 81% while maintaining full specificity (Fig. S1*D*). Fatigue or depression could be excluded to confound the results, as none of the patients was found to show symptoms of depression (Table S1). and the level of cognitive efficiency was unrelated to any metric of the Modified Fatigue Impact Scale (33) (Fig. S1*E*).

Taken together, we find cognitive impairment to be a prevailing feature in early stages of MS. The impairment exhibited a salient pattern across patients in the form of a general factor, suggestive of widespread network dysfunctions. In the following we investigated how this behavioral decline manifested itself in structural and functional changes of the CNS.

Structural Damage. To evaluate the structural damage that underlies the observed behavioral impairment, we quantified the relation of cognitive efficiency to several anatomical parameters. For each participant we obtained estimates of the volume of the peripheral gray matter and ventricular cerebrospinal fluid from the structural scans. The volumes of these structures are sensitive markers of atrophy processes. Additionally, we derived maps of fractional anisotropy and mean diffusivity from the diffusion-weighted imaging data. These diffusion parameters indicate the integrity of highly organized tissue, such as the white matter, and allow for an assessment of even subtle disturbances. The strongest association was found within the diffusion parameters. Cognitive efficiency strongly correlated with a distributed pattern of fractional anisotropy (Fig. 2*A*) in the corpus callosum and immediately surrounding structures (see Fig. S2 for mean diffusivity). The atrophy markers did show a considerably weaker relation (Fig. 2*B*). Indeed, the diffusion tensor parameters kept significant predictive power on the level of cognitive efficiency,

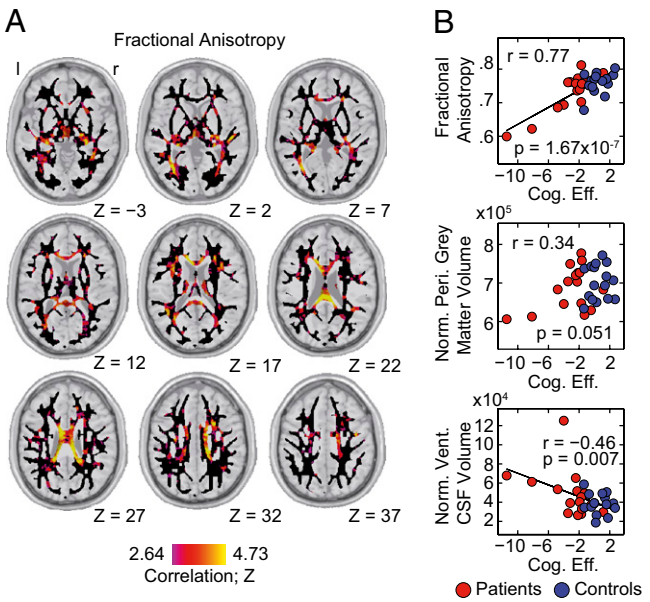

Fig. 2. The loss of cognitive efficiency relates to widespread structural damage. (*A*) Group-level correlation of cognitive efficiency with voxel-wise fractional anisotropy. The analysis was performed within a standard-space white matter mask shown as a black underlay. Correlations are shown as corresponding z-scores and have been thresholded at $P = 0.05$, FDR corrected. No negative correlations passing this threshold were observed. (*B*) The relation of cognitive efficiency to three anatomical parameters: (*Top*) mean fractional anisotropy within a corpus callosum mask, (*Middle*) volume of the peripheral gray matter normalized for individual head size, and (*Bottom*) normalized volume of the ventricular cerebrospinal fluid. Patients are shown as red dots; healthy controls are shown as blue dots.

NEUROSCIENCE

even when removing the most extreme patients from the analysis or performing the analysis only within the patient group (Fig. S2). These results suggest the level of cognitive efficiency to strongly relate to structural damage as reflected in a broadly distributed pattern of reduced white matter integrity.

Functional Connectivity Modulations. We studied the changes in functional connectivity that are related to cognitive efficiency with a data-driven procedure (Fig. 3*A* and *Materials and Methods*). First, we derived measures of connectivity based on the covariation of BOLD time series between ~40,000 voxels that span the cortex for each participant. Then, we quantified the behavioral modulation of functional connectivity by correlating the strength of each connection with cognitive efficiency across participants. We used random permutation statistics to identify voxels that had a modulation in connectivity (see Fig. 3*A*, Fig. S3, and *SI Materials and Methods* for a detailed description of the method). This procedure identified distributed sets of voxels [$n = 447$, $P < 0.05$, false discovery rate (FDR) corrected] that exhibited significant modulation (Fig. 3*B*). The largest clusters of behavioral modulation localized to bilateral inferior parietal cortices as well as to midline structures in the posterior cingulate and medial frontal cortex (Table S2). Importantly, the procedure did not make any assumptions about specific functional networks or whether connectivity increases or decreases contribute to the modulation. In other words, these regions changed their connectivity, but the spatial patterns of these connectivity changes, as well as the direction in which the connectivity was changed (increase or decrease), remained unresolved by this first analysis step.

The spatial patterns underlying the behavioral modulation can be revealed from the individual modulation profiles of each of the identified voxels. The modulation profile contains the global increases and decreases of connectivity with cognitive efficiency. First, we analyzed whether the 447 modulation profiles exhibited similarity across voxels. Indeed, the similarity matrix revealed a strong dominance by one underlying pattern (Fig. 4*A*). Two groups of voxels emerged that were characterized by a highly similar modulation profile within the group and an inverted pattern between the groups. We then derived the underlying dominant spatial pattern of modulation as the first principal component of the modulation profiles (Fig. 4*B*). This dominant spatial pattern explained 40.4% of the total modulation variance and comprised two functional networks: (*i*) the default mode network (DMN; negative values) and (*ii*) areas implicated in the deployment of attention and cognitive control, hereafter referred to as the control network (CN; positive values) (34). The networks' opposite sign indicated that the major connectivity modulation was a concurrent increase of connectivity to one network and a decrease of connectivity to the other. We then further analyzed the strength with which each of the 447 voxels expressed this dominant pattern of modulation (Fig. 4*C*). Rendering the loadings of the dominant modulation pattern on the cortical surface again revealed the two groups of voxels, which exhibited the pattern in an inverted way. The larger group was located in the bilateral parietal cortices, posterior cingulate cortex, and medial prefrontal cortex. These structures spatially overlapped with core parts of the DMN. The positive loadings of these regions showed them to exhibit the modulation pattern as depicted in Fig. 4*B*. Connectivity was shifted toward the DMN in cognitively less-efficient participants (anticorrelation), whereas it was shifted toward the CN in cognitively efficient participants (positive correlation). The smaller cluster exhibited the same pattern of modulation, but connectivity was shifted in the opposite way between the networks (negative loadings). These structures, spatially corresponding to parts of the CN, showed a connectivity shift toward the CN in cognitively less-efficient participants, and a connectivity shift toward the DMN in cognitively efficient participants. Thus, the spatially distributed modulations of functional connectivity involved two major functional networks, the DMN and CN. The nature of the modulations was a shift of connectivity toward the spatially corresponding network in cognitively less-efficient participants and, at the same time, away from the other network.

An increase in BOLD time-course correlations (connectivity) could reflect a change from moderately positive to highly positive correlation values in the patients, but also a change from strong anticorrelation toward less anticorrelation. The important difference between these scenarios cannot be revealed from the modulation alone. In a last step, we thus went back to the first level of analysis and mapped the actual range of connectivity that was underlying the modulations. To this end we constructed a connectivity graph between the two groups of identified regions (Fig. 4*C*) and the two networks of the dominant spatial modulation pattern (Fig. 4*B* and *SI Materials and Methods*). We then derived the average within- and across-network connectivity. The within-network connectivity increased toward more positive correlation values in the patients (Fig. 4 *D* and *E*). For both groups the average within-network connectivity was significantly positive (DMN: patient group, *t* test, $P = 8.5 \times 10^{-5}$, control group, *t* test, $P = 7 \times 10^{-7}$; CN: patient group, *t* test, $P = 2.6 \times 10^{-6}$, control group, *t* test, $P < 1 \times 10^{-7}$), with the patient group showing a higher connectivity (DMN: paired *t* test, $P = 0.035$; CN: paired *t* test, $P = 0.022$). The finding that the control group exhibited positive connectivity suggested that the identified regions were loosely associated with the networks in the healthy condition and became integrated more strongly in the patient group.

The two networks involved in these modulations have previously been shown to exhibit an intrinsically anticorrelated relationship during rest (35) as well as in task situations (36). In agreement with these findings, for both networks the increased connectivity was accompanied by a more marked anticorrelation with the other network. The average across-network correlations were negative for both groups (Fig. 4*F*; patient group *t* test, $P = 0.0017$, control group *t* test, $P = 7 \times 10^{-4}$), with the patients exhibiting stronger anticorrelations (paired *t* test, $P = 0.037$).

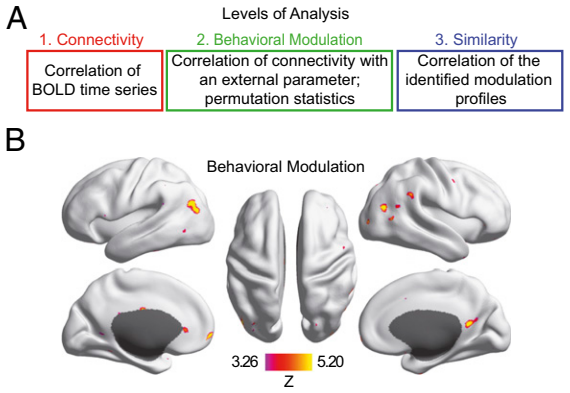

Fig. 3. Functional connectivity is modulated by the level of cognitive efficiency. (*A*) Three levels of the fMRI data analysis stream build upon each other. The colored frames correspond with the more detailed depiction in Fig. S3. Based on the global connectivity between all voxel pairs, we calculated the correlation of all connections with cognitive efficiency across participants. This calculation resulted in a global modulation matrix in which each row (modulation profile) represented the increases and decreases of connectivity that occurred in association with the level of cognitive efficiency for a given voxel. We assessed the statistical significance of the modulation by permutation statistics (*SI Materials and Methods* and Fig. S3). To further investigate the effect, we calculated the similarity matrix of the identified modulation profiles (Fig. 4*A*) in subsequent analyses. This matrix represents the cross-correlations of all of the identified modulation profiles. (*B*) Cortical regions, which exhibit significant modulation by cognitive efficiency. The map has been thresholded at $P = 0.05$, one-tailed, FDR corrected.

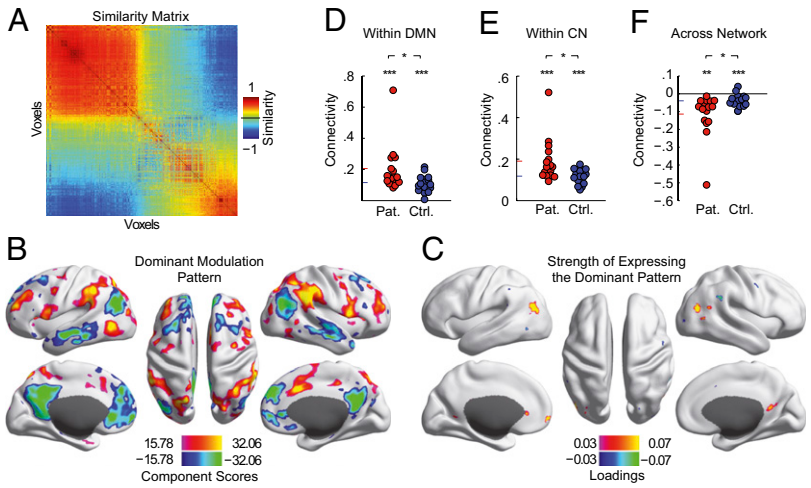

Fig. 4. Increased functional connectivity marks the severity of the cognitive pathology. (*A*) Similarity matrix of the modulation profiles (n = 447; cf. Fig. 3*B*). (*B*) The dominant spatial pattern of connectivity modulations explaining 40.4% of the overall connectivity modulation variance. The color range is set to show the top 25% of absolute values. (*C*) Voxel-wise principal PCA loadings indicating how strongly and with which sign each of the identified regions expressed the spatial pattern of connectivity modulations shown in *B*. The color range is set to show the top 75% of absolute values. (*D–F*) Average cross-connectivity between the two clusters of identified regions and the two networks of the dominant spatial modulation pattern (*SI Materials and Methods*). Group means are indicated by colored bars at the ordinate.

Note that the statistics shown in Fig. 4 *D–F* are not independent from the procedure, which identified the effect. The existence of group differences in the connectivity data underscores the robustness of the effect but had to be expected from the nature of the behavioral parameter. The focus of analysis here was the range of actual connectivity that is spanned by the modulations. To control whether the two most extreme cases in the patient group could have driven these results alone, we performed control analyses without them (Fig. S4*C*). Both the association of connectivity with behavior as well as the group differences were present when omitting these patients. Additional control analyses regarding the preprocessing of the fMRI data and head movement levels are detailed in *SI Materials and Methods*.

Taken together, the pathological loss of cognitive efficiency was associated with a gain of functional connectivity among core parts of the default mode network as well as a control network. These effects distinguished the groups and got stronger as the cognitive impairment and thus structural damage worsened.

Discussion

We have investigated the relation of a salient, pathological pattern in behavior to the covariance structure of spontaneous brain activity in patients with early stage MS. At the heart of our observations lies the divergent role of anatomical and functional connectivity measures in indexing the level of cognitive ability. Functional connectivity within two networks increased in the face of a concomitant reduction of anatomical connectivity and a decline in cognitive efficiency. This finding seemingly contradicts the predominant view of how functional connectivity indexes the integrity of the underlying circuits. A gain in shared variance of the BOLD fluctuations is often interpreted as a gain in functional interactions between the brain regions. Conversely, a pathological loss of function is thought to be reflected in a loss of cofluctuations in dedicated brain systems. This view has been supported by numerous studies across diverse neurological conditions, such as stroke (6, 37), traumatic brain injury (38), Alzheimer's disease (39), vegetative state and coma (40), callosotomy (20), and the decline in healthy aging (8), raising the question of what may be different in the case of MS.

Several of our observations suggest that a main distinct feature of the pathology may be the diffuse and distributed impact MS has on white matter integrity and CNS networks. First, the behavioral parameter, which was used to identify the connectivity modulations, exhibited a notable multivariate structure. The appearance of a general factor suggests a loss of resources, which are required to support a sufficient bandwidth of cognitive processes, conjointly affecting otherwise more distinct cognitive domains (Fig. S1*F*). Second, we find the strongest association between the level of cognitive efficiency and structural measures in a spatially widespread pattern of white matter integrity. And third, the increased connectivity was present in networks implied in different cognitive functions, such as cognitive control of external (41, 42) and internal information (34, 36, 43–45). These networks are commonly recruited across a wide variety of cognitive tasks, and require the coordinated flow of information across a wide expanse of cortex, supported by long-range fiber tracts. Thus, all aspects of our analyses coherently point to a diffuse and widespread impact of the disease on CNS functioning.

With these considerations in mind, there may be two major lines of argument for assigning physiological significance to the increased functional connectivity. First, cortical plasticity processes may be central to our results. A well-replicated finding in task activation studies is that patients in various stages of the disease will show an enhanced recruitment of task-relevant areas (46–49). These effects specifically involve an extension of the activation patterns to additional and functionally related brain areas. Such results are commonly interpreted as indicating an increased neural effort in cortical computation due to the presence of structural damage. Our observations could thus reflect the traces of these repetitive and increased coactivations, with the functional connectivity tracking the statistical history of coactivation in cortical circuits. A number of recent studies in healthy subjects have documented the strengthening of functional connectivity with training-induced improvement in functions in multiple domains, including the motor (2), visual (3), and mnemonic system (4). Thus, increased functional connectivity could provide a compensatory mechanism that, through Hebbian plasticity, limits the consequences of neurological damage and helps to maintain a viable level of computational capacity. However, this putative compensatory function does not agree well with the negative relationship between functional connectivity and cognitive abilities as reported here. Enhanced plasticity

might, in principle, also be maladaptive and directly contribute to the worsening of cognitive functions.

An alternative explanation would be that the reduction in white matter integrity may have led to a loss of diversity in large-scale cortical dynamics. The finding of widespread structural disturbances suggests that the pathological process may have strongly reduced the anatomical basis for functional interactions in a diffuse manner. Instead of specific connectivity being lost completely, the identified regions of modulation might hereby have lost flexibility in their functional interactions. With progressing severity, the regions would be unable to gear up to more variable states and thus more frequently participate in prevalent global patterns of activity (DMN, CN), which would result in stronger apparent connectivity on long time-scales resulting from the more rigid and less-differentiated patterns of functional connectivity. Such a loss-of-diversity account also fits well with reduced cognitive efficiency as the major neuropsychological consequence, suggesting that less-diverse patterns of functional connectivity may be a correlate of the reduced bandwidth of cognitive processes. These arguments share conceptual similarity with the process of dedifferentiation during aging, in which cognitive representations such as receptive fields get gradually less specific and more broadly tuned (50, 51). Increased functional connectivity reflecting a loss of diversity in interactions may indeed be a phenomenon common to pathologies in which a diffuse reduction, but not the absence, of anatomical connectivity is a prevalent feature. Recent converging lines of theoretical work further support this view. Here the functional dynamics are seen as an exploration of possible states upon a static structural scaffold (52). The hypothesis of a loss of possible interactions within this scaffold naturally reconciles the seemingly divergent role of anatomical and functional connectivity in indexing the level of cognitive ability. However, given the available data, these considerations so far remain hypothetical. Our observations call for theoretical studies addressing the effects of gradual and diffuse, instead of complete and focal, ablations in the cortical connectivity regime on the organization of the unfolding functional dynamics.

Overall, our findings show an association of increased functional connectivity in distinct systems with decreased cognitive ability in MS. These observations were made without assumptions regarding specific brain systems and by means of a careful consideration of the prevailing cognitive impairment. The functional connectivity analysis was entirely data driven and based on the hypothesis that the behavioral parameter derived from the neuropsychological testing is informative about individual CNS integrity. Our approach took advantage of the strong pathological variability in the patient data, which may render mean-based approaches such as group comparisons insensitive, and thus represents a valuable procedure in revealing pathophysiological principles in functional imaging data. Our findings extend recent observations, which have been made using independent component analysis, of spontaneous brain activity in MS. These studies have reported on increased synchronization measures of network patterns in different stages of the disease (21–23), but the exact relation to individual behavioral status had remained unclear. Changes of functional networks and their large-scale dynamics may provide a key level of description for understanding how MS affects the CNS. Future studies will be needed to characterize the stage of white matter disintegration that marks the transition from increased functional connectivity to reductions in coupling and the eventual complete absence of cofluctuations (18–23). Our findings suggest that incorporating subtle estimates of the individual behavioral state in addition to contrasts between clinically defined groups is an important element when investigating the impact of MS on brain networks.

Materials and Methods

A detailed description of the applied methods is given in *SI Materials and Methods*. In the following we give a brief account of our procedures.

Study Design. Sixteen early stage MS patients and 16 healthy controls matched for age, sex, and education participated in the experiments (*SI Materials and Methods* and Table S1). Each participant completed three experimental stages within 1–4 successive days: (*i*) neuropsychological examination with a battery of self-evaluation and cognitive measures; (*ii*) 20-min recording of magnetencephalography (275-channel CTF MEG System) during silent fixation; and (*iii*) MRI session, with a recording of ~20 min BOLD signal during silent fixation and high-resolution anatomical as well as diffusion-weighted images. The local ethics committee approved the study, and each study participant gave informed consent before taking part in the experiments. All experiments were conducted according to the Declaration of Helsinki.

Data Analysis. The analysis of the behavioral data was performed on 10 cognitive measures, which were extracted from the more demanding parts of the tests. The raw scores were normalized with the appropriate normative data of a healthy population, matching the individual participants in age and education. The behavioral parameter "cognitive efficiency" was then estimated as the first principal component of the resulting performance matrix containing all normalized test results of all participants. The analysis of the structural damage was done using FSL (http://www.fmrib.ox.ac.uk/fsl/) (53). The diffusion tensor parameters were estimated with the diffusion-weighted imaging tools as documented in the initial steps of TBSS (http://www.fmrib.ox.ac.uk/fsl/tbss/index.html) (54). Statistical analyses were performed within a standard-space white matter mask (FMRIB58_FA skeleton thresholded at 0.2), shown as a black underlay in Fig. 2*A* and Fig. S2*A*. The tissue volumes (normalized for individual head size) were calculated using SIENAX (55). The global modulation of functional connectivity by the level of cognitive efficiency was calculated after standard preprocessing procedures of the functional data. In short, for each voxel, the behavioral modulation of functional connectivity was calculated as the number of significant ($P = 0.01$, uncorrected) group-level correlations that occurred between its global connectivity pattern and the level of cognitive efficiency. For assessing the statistical significance of the modulations, the procedure was repeated 100× while randomly permuting the behavioral parameter. A normal distribution was fitted to these resamples to derive an empirical distribution for the null hypothesis of no connectivity modulation with cognitive efficiency. This distribution was used to derive z-scores (subtraction of mean and division by the SD) and *P* values. We corrected for multiple statistical testing by controlling for the FDR (56).

ACKNOWLEDGMENTS. We thank all patients who participated in these experiments. We also thank Roland Martin, Sven Schippling, and the team of the Institute for Neuroimmunology and Clinical MS Research at the Department of Neurology of the University Medical Center Hamburg-Eppendorf for support. This work was supported by European Union Grant HEALTH-F2-2008-200728, BrainSync.

1. Fox MD, Raichle ME (2007) Spontaneous fluctuations in brain activity observed with functional magnetic resonance imaging. *Nat Rev Neurosci* 8:700–711.
2. Albert NB, Robertson EM, Miall RC (2009) The resting human brain and motor learning. *Curr Biol* 19:1023–1027.
3. Lewis CM, Baldassarre A, Committeri G, Romani GL, Corbetta M (2009) Learning sculpts the spontaneous activity of the resting human brain. *Proc Natl Acad Sci USA* 106:17558–17563.
4. Tambini A, Ketz N, Davachi L (2010) Enhanced brain correlations during rest are related to memory for recent experiences. *Neuron* 65:280–290.
5. Dosenbach NUF, et al. (2010) Prediction of individual brain maturity using fMRI. *Science* 329:1358–1361.
6. He BJ, et al. (2007) Breakdown of functional connectivity in frontoparietal networks underlies behavioral deficits in spatial neglect. *Neuron* 53:905–918.
7. Seeley WW, Crawford RK, Zhou J, Miller BL, Greicius MD (2009) Neurodegenerative diseases target large-scale human brain networks. *Neuron* 62(1):42–52.
8. Damoiseaux JS, et al. (2008) Reduced resting-state brain activity in the "default network" in normal aging. *Cereb Cortex* 18:1856–1864.
9. Hagmann P, et al. (2008) Mapping the structural core of human cerebral cortex. *PLoS Biol* 6:e159.
10. Skudlarski P, et al. (2008) Measuring brain connectivity: Diffusion tensor imaging validates resting state temporal correlations. *Neuroimage* 43:554–561.

11. Honey CJ, et al. (2009) Predicting human resting-state functional connectivity from structural connectivity. *Proc Natl Acad Sci USA* 106:2035–2040.
12. Alstott J, Breakspear M, Hagmann P, Cammoun L, Sporns O (2009) Modeling the impact of lesions in the human brain. *PLOS Comput Biol* 5:e1000408.
13. Honey CJ, Sporns O (2008) Dynamical consequences of lesions in cortical networks. *Hum Brain Mapp* 29:802–809.
14. Corbetta M (2010) Functional connectivity and neurological recovery. *Dev Psychobiol*, 10.1002/dev.20507.
15. Honey CJ, Thivierge J-P, Sporns O (2010) Can structure predict function in the human brain? *Neuroimage* 52:766–776.
16. Zhang D, Raichle ME (2010) Disease and the brain's dark energy. *Nat Rev Neurol* 6(1): 15–28.
17. Compston A, Coles A (2008) Multiple sclerosis. *Lancet* 372:1502–1517.
18. Lowe MJ, et al. (2002) Multiple sclerosis: Low-frequency temporal blood oxygen level-dependent fluctuations indicate reduced functional connectivity initial results. *Radiology* 224(1):184–192.
19. Rocca MA, et al. (2010) Default-mode network dysfunction and cognitive impairment in progressive MS. *Neurology* 74:1252–1259.
20. Johnston JM, et al. (2008) Loss of resting interhemispheric functional connectivity after complete section of the corpus callosum. *J Neurosci* 28:6453–6458.
21. Roosendaal SD, et al. (2010) Resting state networks change in clinically isolated syndrome. *Brain* 133:1612–1621.
22. Valsasina P, et al. (2011) A multicentre study of motor functional connectivity changes in patients with multiple sclerosis. *Eur J Neurosci* 33:1256–1263.
23. Bonavita S, et al. (2011) Distributed changes in default-mode resting-state connectivity in multiple sclerosis. *Mult Scler* 17:411–422.
24. Chiaravalloti ND, DeLuca J (2008) Cognitive impairment in multiple sclerosis. *Lancet Neurol* 7:1139–1151.
25. Filippi M, et al. (2010) The contribution of MRI in assessing cognitive impairment in multiple sclerosis. *Neurology* 75:2121–2128.
26. Barkhof F (2002) The clinico-radiological paradox in multiple sclerosis revisited. *Curr Opin Neurol* 15:239–245.
27. Filippi M, et al. (2000) Changes in the normal appearing brain tissue and cognitive impairment in multiple sclerosis. *J Neurol Neurosurg Psychiatry* 68(2):157–161.
28. Dineen RA, et al. (2009) Disconnection as a mechanism for cognitive dysfunction in multiple sclerosis. *Brain* 132:239–249.
29. Mesaros S, et al. (2009) Corpus callosum damage and cognitive dysfunction in benign MS. *Hum Brain Mapp* 30:2656–2666.
30. Roosendaal SD, et al. (2009) Regional DTI differences in multiple sclerosis patients. *Neuroimage* 44:1397–1403.
31. Filippi M, Rocca MA (2005) MRI evidence for multiple sclerosis as a diffuse disease of the central nervous system. *J Neurol* 252(Suppl 5):v16–v24.
32. Duncan J (2010) The multiple-demand (MD) system of the primate brain: Mental programs for intelligent behaviour. *Trends Cogn Sci* 14(4):172–179.
33. Zimmermann C, Hohlfeld R (1999) "Fatigue" in multiple sclerosis (Translated from German). *Nervenarzt* 70:566–574.
34. Raichle ME (2010) Two views of brain function. *Trends Cogn Sci* 14(4):180–190.
35. Fox MD, et al. (2005) The human brain is intrinsically organized into dynamic, anti-correlated functional networks. *Proc Natl Acad Sci USA* 102:9673–9678.
36. Sestieri C, Shulman GL, Corbetta M (2010) Attention to memory and the environment: Functional specialization and dynamic competition in human posterior parietal cortex. *J Neurosci* 30:8445–8456.
37. Carter AR, et al. (2010) Resting interhemispheric functional magnetic resonance imaging connectivity predicts performance after stroke. *Ann Neurol* 67:365–375.
38. MacDonald CL, et al. (2008) Verbal memory deficit following traumatic brain injury: Assessment using advanced MRI methods. *Neurology* 71:1199–1201.
39. Greicius MD, Srivastava G, Reiss AL, Menon V (2004) Default-mode network activity distinguishes Alzheimer's disease from healthy aging: Evidence from functional MRI. *Proc Natl Acad Sci USA* 101:4637–4642.
40. Vanhaudenhuyse A, et al. (2010) Default network connectivity reflects the level of consciousness in non-communicative brain-damaged patients. *Brain* 133(Pt 1): 161–171.
41. Corbetta M, Shulman GL (2002) Control of goal-directed and stimulus-driven attention in the brain. *Nat Rev Neurosci* 3:201–215.
42. Dosenbach NU, Fair DA, Cohen AL, Schlaggar BL, Petersen SE (2008) A dual-networks architecture of top-down control. *Trends Cogn Sci* 12(3):99–105.
43. Buckner RL, Andrews-Hanna JR, Schacter DL (2008) The brain's default network: Anatomy, function, and relevance to disease. *Ann N Y Acad Sci* 1124:1–38.
44. Shulman GL, et al. (1997) Common blood flow changes across visual tasks: II. Decreases in cerebral cortex. *J Cogn Neurosci* 9:648–663.
45. Raichle ME, et al. (2001) A default mode of brain function. *Proc Natl Acad Sci USA* 98: 676–682.
46. Audoin B, et al. (2003) Compensatory cortical activation observed by fMRI during a cognitive task at the earliest stage of MS. *Hum Brain Mapp* 20(2):51–58.
47. Pantano P, et al. (2002) Cortical motor reorganization after a single clinical attack of multiple sclerosis. *Brain* 125:1607–1615.
48. Rocca MA, et al. (2005) Cortical adaptation in patients with MS: A cross-sectional functional MRI study of disease phenotypes. *Lancet Neurol* 4:618–626.
49. Loitfelder M, et al. (2011) Reorganization in cognitive networks with progression of multiple sclerosis: Insights from fMRI. *Neurology* 76:526–533.
50. Park DC, et al. (2004) Aging reduces neural specialization in ventral visual cortex. *Proc Natl Acad Sci USA* 101:13091–13095.
51. Goh JOS (2011) Functional dedifferentiation and altered connectivity in older adults: Neural accounts of cognitive aging. *Aging Dis* 2(1):30–48.
52. Deco G, Jirsa VK, McIntosh AR (2011) Emerging concepts for the dynamical organization of resting-state activity in the brain. *Nat Rev Neurosci* 12(1):43–56.
53. Smith SM, et al. (2004) Advances in functional and structural MR image analysis and implementation as FSL. *Neuroimage* 23(Suppl 1):S208–S219.
54. Smith SM, et al. (2006) Tract-based spatial statistics: Voxelwise analysis of multi-subject diffusion data. *Neuroimage* 31:1487–1505.
55. Smith SM, De Stefano N, Jenkinson M, Matthews PM (2001) Normalized accurate measurement of longitudinal brain change. *J Comput Assist Tomogr* 25:466–475.
56. Benjamini Y, Hochberg Y (1995) Controlling the false discovery rate: A practical and powerful approach to multiple testing. *J R Stat Soc B* 57:289–300.